

P. HANDZLIK*, K. FITZNER*

SEMICONDUCTING PROPERTIES OF ANODIC OXIDE FILMS GROWN ON TITANIUM IN RINGER AND PBS SOLUTIONS

WŁAŚCIWOŚCI PÓŁPRZEWODNIKOWE ANODOWYCH WARSTW TLENKOWYCH OTRZYMANÝCH NA TYTANIE W ROZTWORZE RINGERA I SOLI FIZJOLOGICZNEJ BUFOROWANEJ FOSFORANAMI

In the present study investigations of semiconducting properties of anodic oxide films formed on titanium were carried out. Oxide films were produced by using potentiostatic anodization of the metal in two solutions: PBS solution with pH = 8.9 and Ringer solution with pH = 7.8. In order to analyze the properties of the obtained films, Electrochemical Impedance Spectroscopy (EIS) was applied. To characterize the surface morphology Scanning Electron Microscopy (SEM) was used. From the results of this study the following properties of the titanium dioxide films were determined: a density of charge carriers and a flat band potential. To derive these parameters Mott-Schottky dependence was applied. Donor densities were found to be of the order of 10^{20} carriers per cm^3 . In turn, average flat band potentials are found to be -0.736 V vs. SCE in Ringer solution and -0.784 V vs. SCE in PBS solution.

Keywords: Titanium, Anodic oxides, Thin films, Impedance spectroscopy, Semiconductivity

W pracy wykonano badania mające na celu określenie właściwości półprzewodnikowych anodowych warstw tlenkowych wytworzonych na tytanie. Warstewki te zostały wytworzone poprzez anodowanie metalu przy stałych potencjałach w następujących dwóch roztworach: roztworze PBS o pH równym 8,9 i roztworze Ringera o pH równym 7,8. Do określenia właściwości tych warstewek użyto Elektrochemicznej Spektroskopii Impedancyjnej. Do przeanalizowania morfologii powierzchni warstw tlenkowych użyto skaningowej mikroskopii elektronowej (SEM). Określono dwie następujące właściwości charakteryzujące warstwy tlenkowe tzn. gęstość nośników ładunku i potencjał płaskiego pasma. Do wyznaczania tych wielkości użyto zależności Motta-Schottky'ego. Stwierdzono, że w zadanych warunkach gęstości donorów są rzędu 10^{20} nośników na cm^3 . Natomiast średnie wartości potencjałów płaskiego pasma wyniosły odpowiednio dla warstw tlenkowych w roztworze PBS: -0.784 V wzgl. NEK, a w roztworze Ringera: -0.736 V wzgl. NEK.

1. Introduction

Titanium and its alloys have been known for their various technological applications mainly in aeronautic technologies due to their not only mechanical but also anti-corrosive properties. Later, passivity of these materials extended their applications into biomedical field where they are being used as dental and orthopedic implants [1]. They are also successfully applied in autoclave liners and internal components where they are subjected simultaneously to severe conditions of acidity, temperature and pressure [2]. This particular corrosion resistance of titanium and its alloys is due to the formation of dense, compact TiO_2 film on the metallic surface. Since, depending on the growth conditions, films grown on the surface may possess different degree of defectness they also exhibit interesting semiconducting properties.

A number of studies [3-11] can be mentioned in which the mechanism of the growth and dissolution of these films in contact with different environments, structure and morphology, charge transfer through the film and transport mechanism as well as the electronic properties were studied. The work of Zwilling *et al* [12] in which it was demonstrated that anodization of titanium may lead to the formation of TiO_2 nanotubes directed the efforts to explore this unusual morphology of films with so large surface areas in new fields of technology. It was found recently that higher concentration of defects is expected in the wall of tubes resulting in higher electronic conductivity of tubular oxides [13]. It was shown that they can be applied in solar cells [14] and in water photolysis [15].

In 1972 Fujishima and Honda [15] described a nov-

* LABORATORY OF PHYSICAL CHEMISTRY AND ELECTROCHEMISTRY, FACULTY OF NON-FERROUS METALS, AGH UNIVERSITY OF SCIENCE AND TECHNOLOGY, 30-059 KRAKÓW, 30 MICKIEWICZA AVE., POLAND

el photo-electrochemical cell which decomposed water using the energy of visible light. Semiconducting n-type TiO₂ was used as the electrode which was irradiated and on which oxygen evolution took place. Thus, it is not surprising that studies of semiconducting properties of TiO₂ films became so important. It was also shown later, that titanium dioxide can be used as excellent photocatalytic material for environmental applications [16]. Recent studies also suggests implant ability to react with blood components (proteins) depend on the ability to charge transfer to the material and variation of semiconducting properties of TiO₂ can be a way for achieving required biological response [17].

Electrochemistry offers an elegant way to determine density of charge carriers in a semiconductor and the flat band potential. It is known that at the solid/electrolyte interface the charges in the solid semiconducting electrode are distributed over a certain thickness called space charge layer. This leads to a positive or negative bending of the energy bands near the surface of the solid electrode. Consequently, the potential difference is established between the bulk and the surface of a semiconductor. This difference can be derived from Mott-Schottky equation [18] which describes the variation of the capacitance of the space charge layer with the potential. The potential of the electrode for which no bending of energy bands occurs is the flat band potential. Blum and Konig used this technique to determine the defect concentration and the flat band potential in TiO₂ as a function of the oxide thickness [19].

In the present paper the flat band potential and donor density in TiO₂ films grown by anodization of titanium in Ringer and PBS aqueous solutions were derived by using Mott-Schottky equation. The aim of this study is to find out if and how these two parameters depend on different environment. Electrochemical impedance spectroscopy (EIS) was used to determine the capacitance of the space charge layer as a function of a given potential.

2. Experimental

2.1. Samples

The specimens were made of titanium rod and sheet (Ti Grade 2 – impurity: O=0.25% max, N=0.03% max, C=0.08% max, H=0.015% max, Fe=0.3% max). They were mechanically polished to a mirror-like surface by a 0.25 μm alumina abrasive. After polishing, they were cleaned with soap and ethanol. Before each experiment they were ultrasonically cleaned in acetone for 10 minutes and then in deionized purified water (Mili Q system, Milipore Corp.) also for 10 minutes. After cleaning the samples were mounted in a PVC holder. The exposed

surface was a circle of 0.283 cm² geometrical area. The roughness factor was about 1.01 as determined from roughness measurements conducted on these samples.

2.2. Cell and electrolytes

Experiments were performed in a three-electrode electrochemical cell containing about 45 cm³ of electrolyte. A platinum wire in the form of a spring was used as a counter electrode. The surface area of counter electrode was equal to 3.3 cm². A saturated calomel electrode (SCE) Radiometer XR100 was the reference electrode and the working electrode was a titanium specimen. Additionally, in all EIS measurements a platinum wire was used. It was immersed in the solution close to the SCE and connected through a capacitor (0.1 - 1 μF) to the reference electrode connector of the potentiostat. This was done to reduce possible problems at high frequencies caused by the reference electrode. The experimental temperature was kept at 21±1°C.

All measurements were performed using the Ringer solution (pH 7.8), and phosphate-buffered saline PBS (pH 8.9). Solutions were prepared from pure analytical-grade compounds supplied by Sigma-Aldrich and deionized purified water (18 MΩ-cm, MiliQ system, Milipore Corp.). The compositions of solutions are presented in Table 1. Electrolytes were not de-aerated to simulate better the conditions of human body fluids. The pH of each solution was measured before and after each experiment using Mettler DL 21 Titrator with the electrode Mettler Toledo DG-111-SC and the value of pH did not change during experiments.

TABLE 1
Composition of the solutions used in experiments

Compound	Concentration in g/dm ³ ± 0.01 g/dm ³	
	Ringer solution pH = 7.8 ± 0.1	PBS pH = 8.9 ± 0.1
NaCl	6.8	8
KCl	0.4	0.2
CaCl ₂	0.2	–
MgSO ₄ ·7H ₂ O	0.2	–
NaH ₂ PO ₄ ·H ₂ O	0.14	–
NaHCO ₃	2.2	–
Na ₂ HPO ₄	–	30
KH ₂ PO ₄	–	0.2
Glucose	1	–

2.3. Experiments

In order to produce TiO₂ films, titanium surface was anodized for 1h at the following potentials: 0.2 V, 1.5

V, 3 V, 5 V, 7 V, 9 V vs. SCE. After each anodization the impedance measurement was performed in order to obtain the capacitance of the film. Also, the native oxide films formed after 1h immersion in solutions were investigated. The EIS measurements were performed on the titanium sample with produced TiO_2 at different potentials from -0.4V to 0.5V with the step 0.1V . At each potential we obtained an impedance spectrum which was measured from 100kHz to 5mHz in the potentiostatic mode using 10mV voltage perturbation. To perform all these measurements Autolab PGSTAT12 was used. From the obtained spectra the capacitance of the film was obtained using to analysis ZView2 software. It was next used to construct Mott-Schottky plots, from which donor densities N_d and flat band potential E_{fb} were calculated.

Samples were examined with SEM (JEOL JSM-5800 LV), operated at 10kV , to characterize the surface morphologies obtained after electrochemical experiments.

3. Results and discussion

An example of potentiodynamic curves is presented in Fig. 1. They have been traced in both solutions mentioned earlier in the range of potentials from -2V to 8V versus SCE with the scan speed 10mV/s . On this basis we have chosen potentials (0.2V , 1.5V , 3V , 5V , 7V , 9V vs. SCE) to form compact oxides on the titanium surface. For potentials marked in this figure by A, B and C surface morphologies of anodized samples were analyzed by SEM and are shown in Fig. 2. Examples of EIS spectra are also shown for these samples. Also, we have obtained the stationary potentials which were measured after one hour of sample immersion in the solution, and these potentials are projected in Fig. 3 on the E-pH diagram given for titanium [20]. As one can see they fall in the passive range, which means that the surface of electrodes should be covered with passive oxide film.

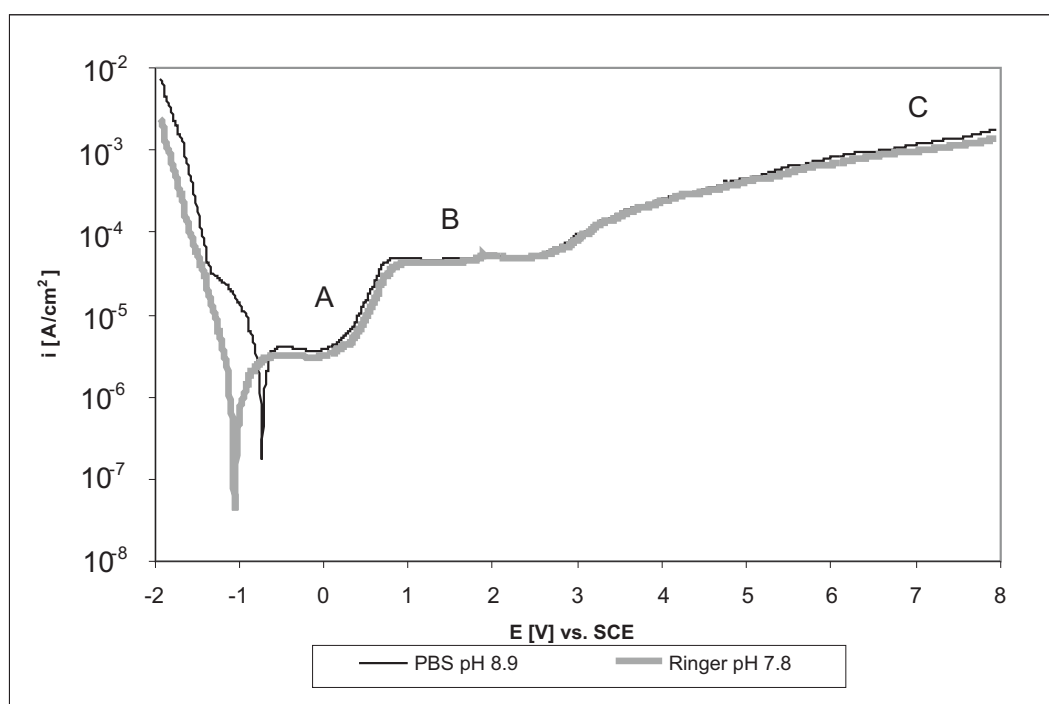


Fig. 1. Potentiodynamic curves obtained for titanium in two different solutions

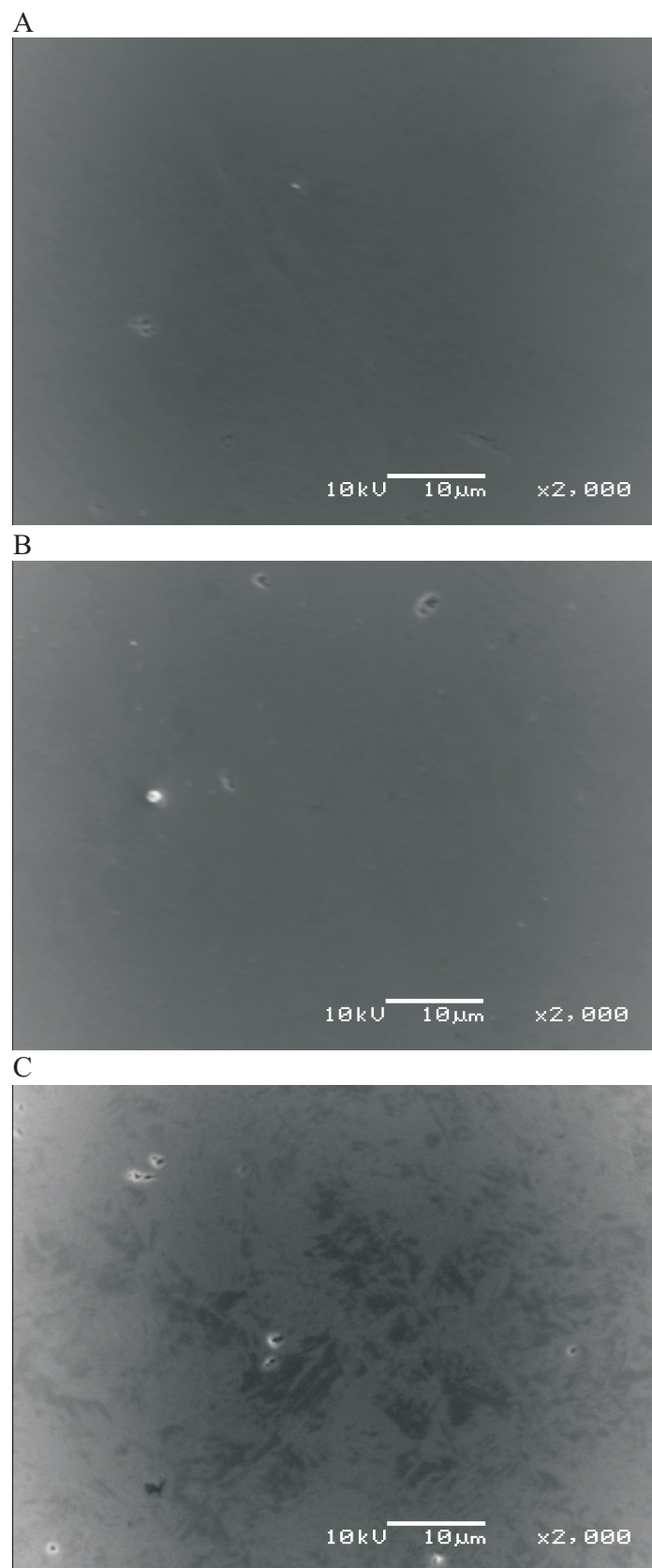


Fig. 2. Examples of surface morphologies obtained after anodic polarization in PBS solution pH=8.9 at the following potentials: A – 0.2V vs. SCE, B – 1.5V vs. SCE, C – 7V vs. SCE which are also depicted in Fig. 1 on potentiodynamic curves

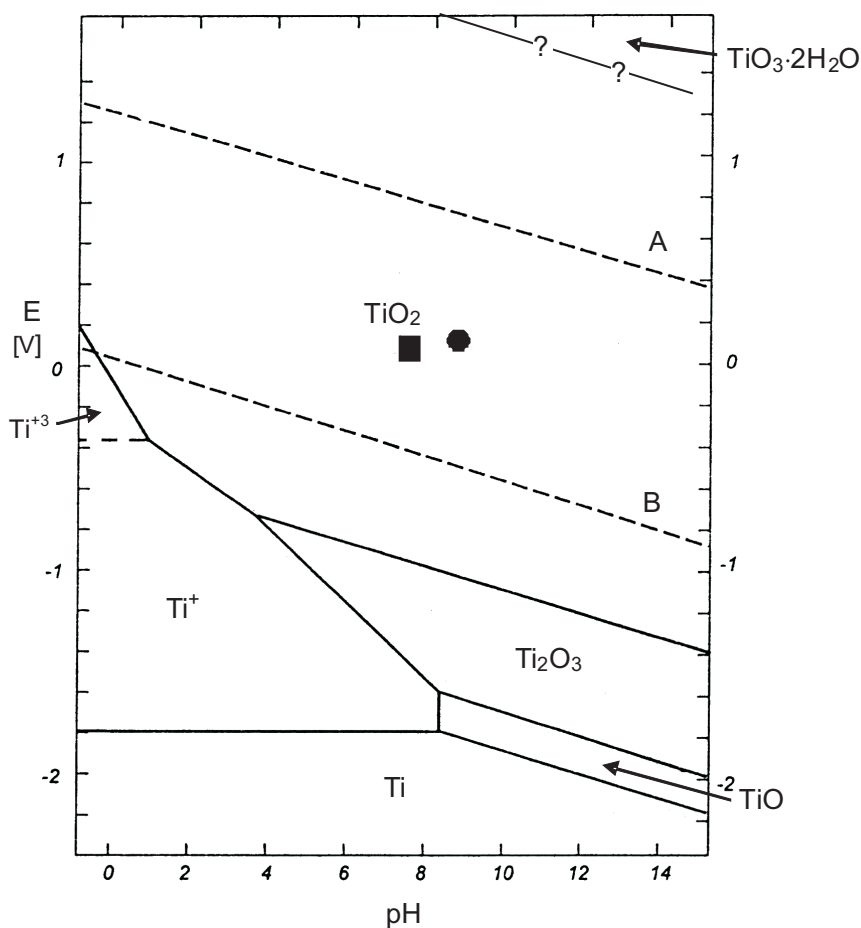


Fig. 3. E-pH diagram for titanium (based on [20]) with the measured stationary potentials (■ – Ringer solution pH = 7.8 and ● – PBS solution pH = 8.9). T = 298K, line A – $\frac{1}{2}O_2 + 2H^+ + 2e^- = H_2O$, line B – $2H^+ + 2e^- = H_2$

The results of EIS measurements carried out on the same samples are presented in Fig. 4 in the form of Nyquist as well as Bode phase plots. From the SEM photos (Fig. 2) we can see that the layer of the oxide film is uniform and flat. The films were amorphous without any

form of crystalline structure. Only the oxide film layers produced at highest potentials (7 V and 9 V vs. SCE) showed some irregularities of surface but this did not prohibit the use of equivalent circuit adopted to analyze the impedance spectra which is shown in Fig. 5.

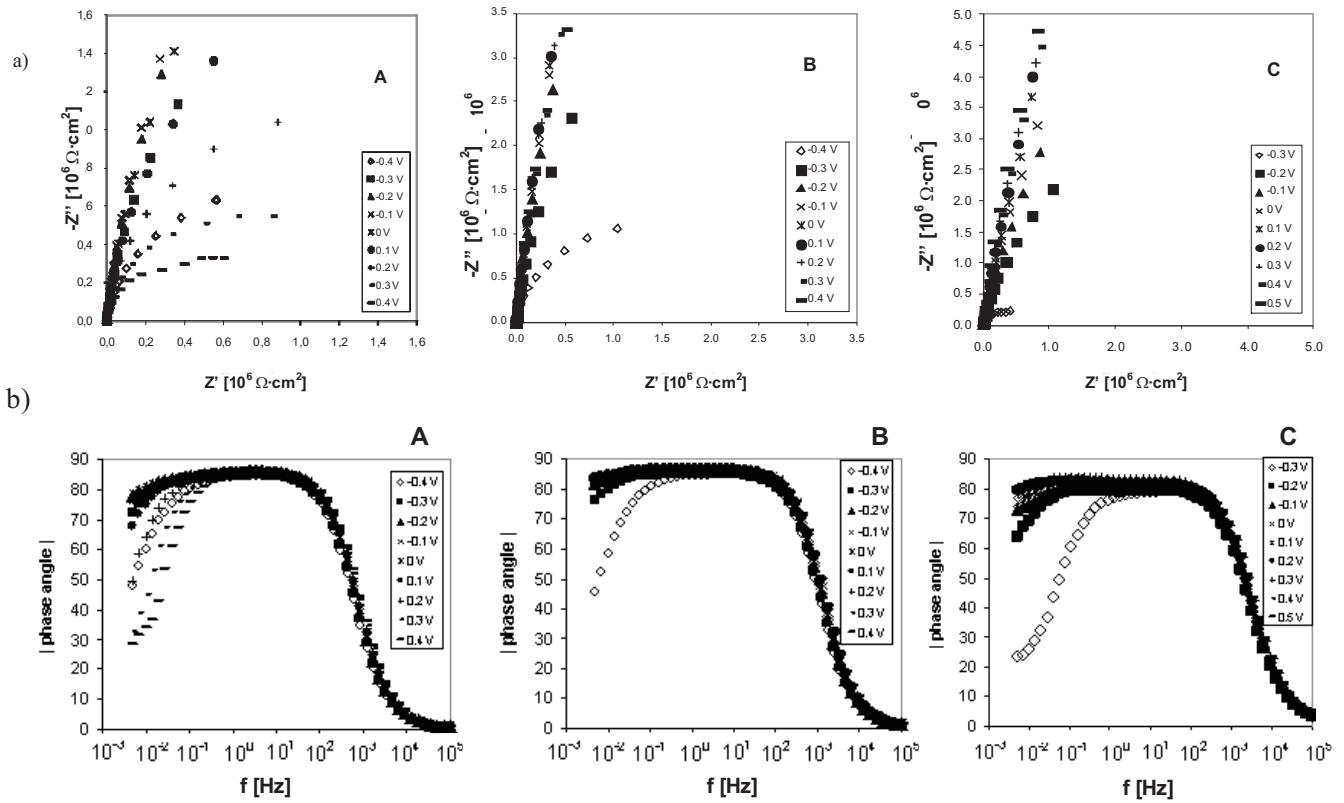


Fig. 4. The results of impedance measurements performed on the TiO₂ films produced in PBS solution pH=8.9 at the following potentials: A – 0.2V vs. SCE, B – 1.5V vs. SCE, C – 7V vs. SCE – a) Nyquist plots, b) Bode phase plots

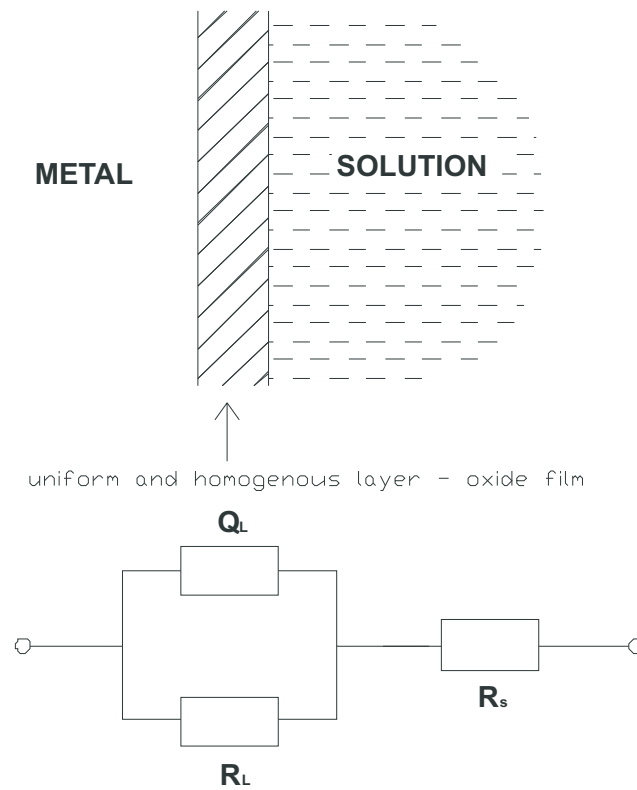


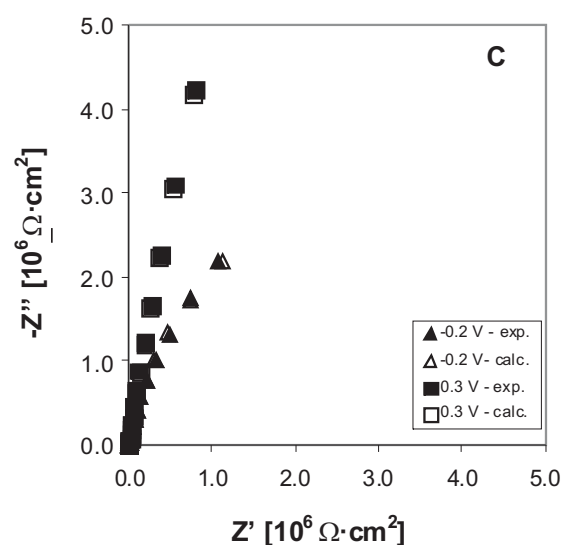
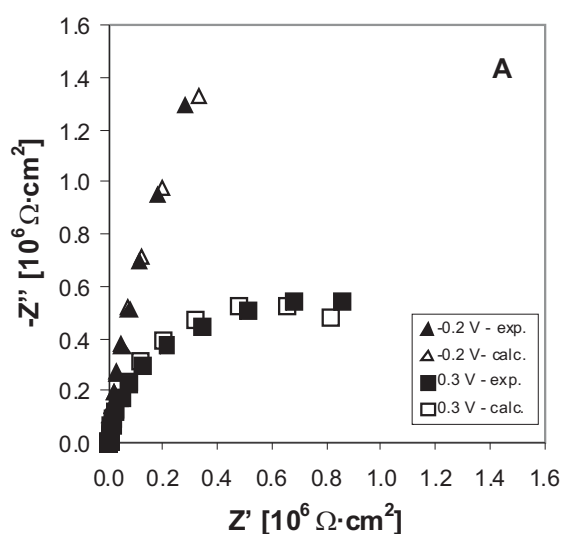
Fig. 5. The model of the metal/oxide/electrolyte interface and electrical equivalent circuit used for analyses of impedance spectra

The CPE (Constant Phase Element) element Q_L was used because the surface of the electrode is never ideally flat and in the electrochemical measurements this element replaces the ideal capacitor [21-23]. The impedance of the CPE element is described by the following formula:

$$Z_Q = \frac{1}{Q(j\omega)^n}, \quad (1)$$

where Q is a pre-exponential factor, which is a frequency-independent parameter; n is the exponent, which defines the character of frequency dependence ($-1 \leq n \leq 1$); $j = \sqrt{-1}$ is the imaginary unit; $\omega = 2\pi f$ [rad·s⁻¹] is angular frequency. With n equal to 1, Q is an ideal capacitance and has the unit of capacitance (F/cm²), in another case when $n \neq 1$, Q has following unit S·s ^{n} /cm².

a)



b)

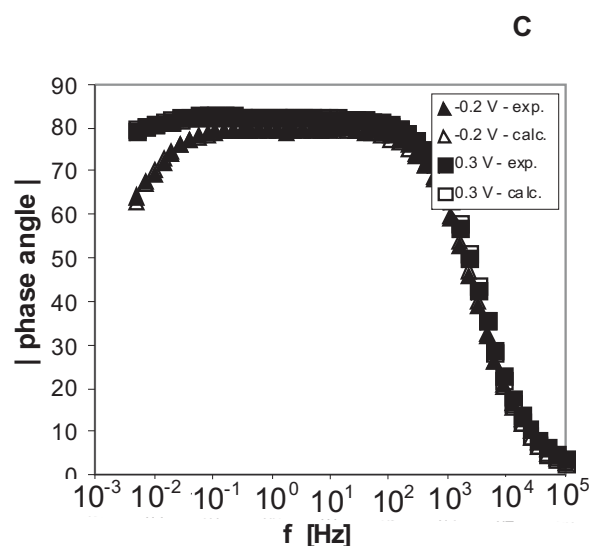
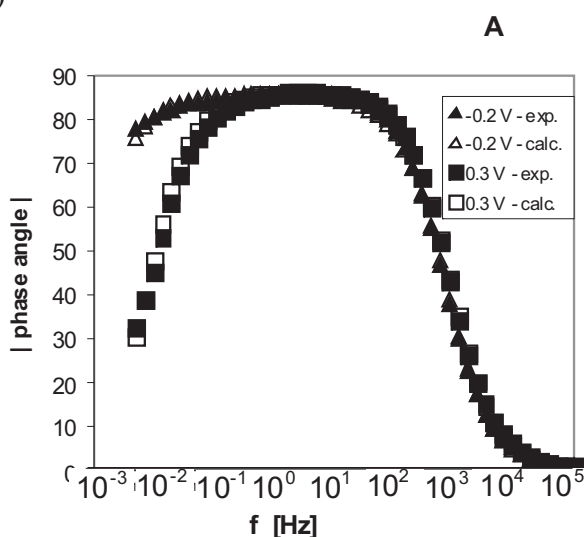


Fig. 6. An example of the comparison of experimental and calculated data taken from analysis of the results of impedance measurements performed on the TiO₂ films produced in PBS solution at the following potentials: A – 0.2V vs. SCE, C – 7V vs. SCE – a) Nyquist plots, b) Bode phase plots

The chi-square tests were used to confirm the correctness of the choice of this equivalent circuit. The values of chi-square are $10^{-3} \div 10^{-4}$ which suggests that the calculated and experimental values are in good agreement. Figure 6 presents examples of experimental and calculated data of the impedance spectra. As one can see the experimental and calculated data are in good agreement indeed, what confirms the right choice of the equivalent circuit. It was found that the Nyquist plots for films formed at other potentials as well as in the Ringer solution also correspond well with this equivalent circuit. Using Nyquist plots and equivalent circuit presented in Fig. 5 the analysis with ZView2 software was performed. Thanks to this procedure the values of R_s , R_L and parameters characterizing the CPE element Q and n were derived. From the point of view of our studies the values of Q and n are essential. Because the values of n varied from 0.91 to 0.96, one can assume that they are equal to 1 and consequently the values of Q were taken as the capacitance C . These values of C were next used to derive Mott-Schottky plots i.e. $1/C^2$ vs. E dependences, which are presented in Fig. 7a and 7b.

The extended Mott-Schottky equation is given below [24]:

$$\frac{1}{C^2} = \frac{2}{e\epsilon\epsilon_0 N_d} \left(E - E'_{fb} - \Delta E - \frac{kT}{e} \right) \approx aE + b \quad (2)$$

$$E_{fb} = E'_{fb} + \Delta E, \quad (3)$$

where:

C – experimental capacity referred to the unit area, e – electron charge = $1.602 \cdot 10^{-19}$ C, ϵ – dielectric constant of TiO_2 , ϵ_0 – electrical vacuum permittivity = $8.85 \cdot 10^{-12}$ F/m, k – Boltzmann constant = $1.38 \cdot 10^{-23}$ J/K, T – temperature, E – experimental potential, E_{fb} – experimental value of flat band potential, E'_{fb} – true flat band potential obtained by correction of E'_{fb} by the potential drop ΔE in the Helmholtz layer, N_d – donor density.

We have used the value of dielectric constant taken from the literature [26] and equal to 50 as an average value for TiO_2 .

Using the Mott-Schottky equation (2) as well as the results shown in Fig. 7a and 7b parameters of linear equations were calculated and from the obtained values of the slope and the intercept donor densities and E'_{fb} values were derived.

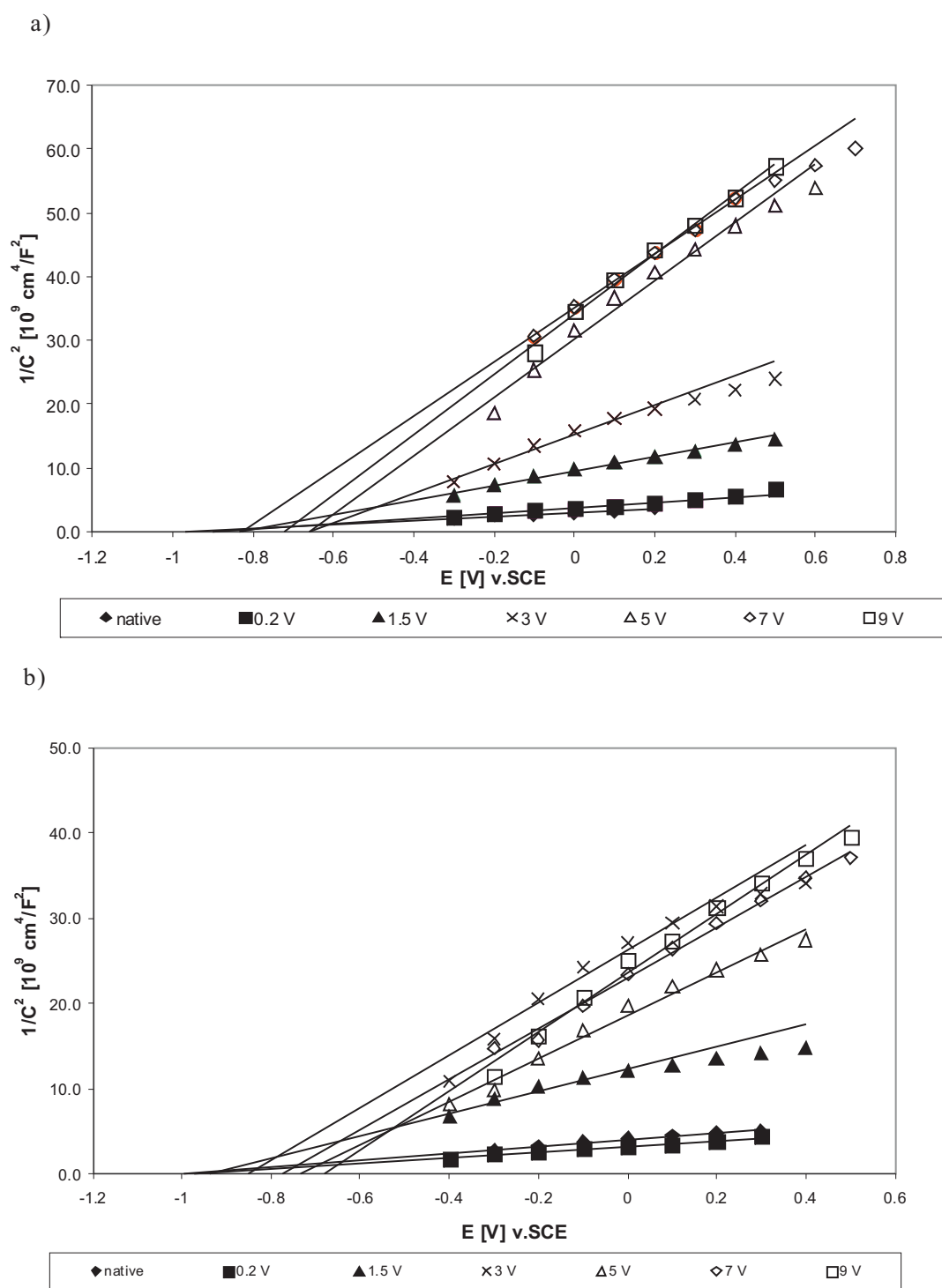


Fig. 7. Mott-Schottky plots for oxides formed at different potentials in a) Ringer solution pH=7.8 and b) PBS pH = 8.9

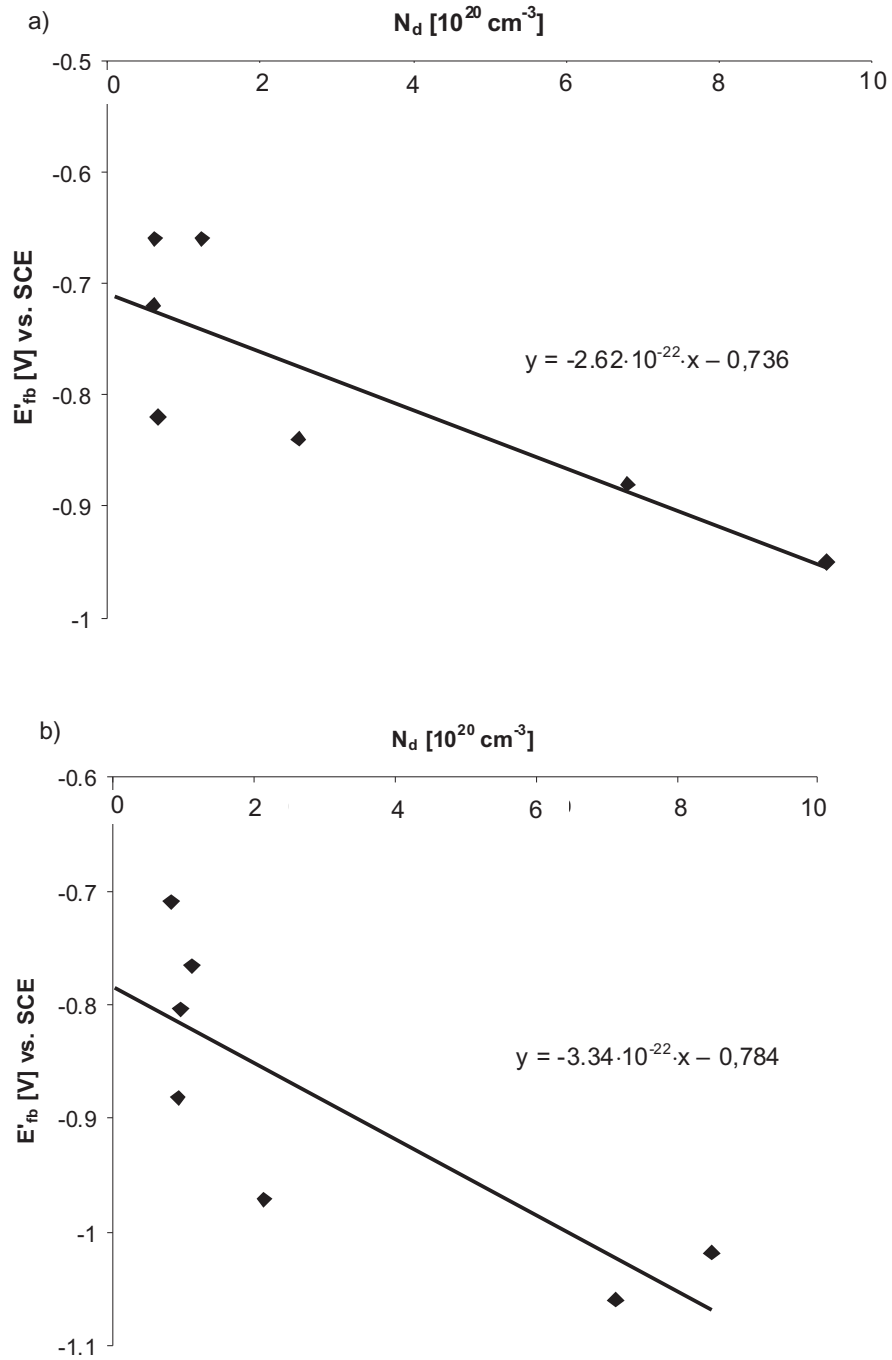


Fig. 8. Dependence $E_{fb} = f(N_d)$ for oxides formed in a) Ringer solution pH=7.8 and b) PBS pH=8.9

Since the true value of the flat band potential given by equation (3) requires the knowledge of the potential drop ΔE in Helmholtz layer which equals $(e\epsilon\epsilon_0 N_d)/(2C_H^2)$. We have first calculated the capacitance of the Helmholtz layer C_H from the dependence $E'_{fb} = f(N_d)$ shown in Fig.8a and 8b.

The slope of this dependence is equal to $(e\epsilon\epsilon_0)/(2C_H^2)$ from which C_H can be calculated. Next, we used these values of C_H to calculate a true value of

the flat band potential. The capacity of the Helmholtz layer was found to be equal about $37 \mu\text{F}/\text{cm}^2$ for Ringer solution and $33 \mu\text{F}/\text{cm}^2$ for PBS solution.

Calculated donor densities, experimental values of the flat band potential and corrected values of the flat band potential are presented in Tables 2a and 2b.

TABLE 2A

The donor densities, the experimental values of the flat band potential, corrected values of the flat band potential for oxides formed in Ringer solution

E [V] vs. SCE	$N_d[1/cm^3] \cdot 10^{20}$	E'_{fb} [V] vs. SCE	E_{fb} [V] vs. SCE
Stationary potential	9.40	-0.978	-0.732
0,2	6.80	-0.908	-0.729
1,5	2.50	-0.866	-0.801
3	1.23	-0.686	-0.654
5	0.62	-0.686	-0.670
7	0.66	-0.851	-0.834
9	0.60	-0.747	-0.732
	average value of E_{fb}		-0.736

TABLE 2B

The donor densities, the experimental values of the flat band potential, corrected values of the flat band potential for oxides formed in PBS solution

E [V] vs. SCE	$N_d[1/cm^3] \cdot 10^{20}$	E'_{fb} [V] vs. SCE	E_{fb} [V] vs. SCE
Stationary potential	7.12	-1.060	-0.822
0,2	8.49	-1.018	-0.735
1,5	2.14	-0.971	-0.900
3	0.92	-0.882	-0.851
5	1.12	-0.766	-0.729
7	0.96	-0.804	-0.772
9	0.82	-0.709	-0.682
	average value of E_{fb}		-0.784

One can notice that donor density is decreasing when the potential of anodization is increasing. The average value of the flat band potential for the oxide formed in Ringer solution is equal to -0.736 V vs. SCE, and for the layer formed in PBS solution it is equal to -0.784 V vs. SCE.

The values calculated from our measurements are comparable with the values of E_{fb} given in other studies [25-27]. In his work [26] Finklea presented the correlation with more than one hundred values of E_{fb} reported in the literature and plot all these data points vs. variable pH. It can be shown that our results correspond well to this correlation (Fig.9).

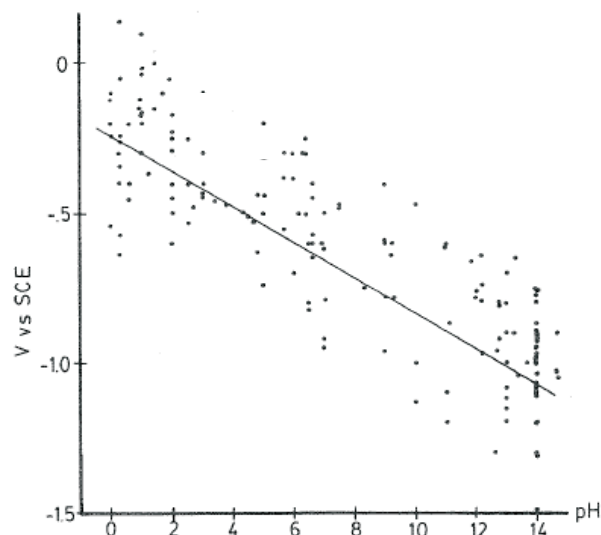


Fig. 9. Reported values of E_{fb} for TiO_2 vs. pH compared with the values obtained in this work (■ – Ringer solution pH=7.8 and ● – PBS solution pH=8.9) and taken from our previous study (□ – PBS solution pH=2.9 and ○ – Artificial saliva pH=5) [28]. The solid line is the standard potential for hydrogen evolution [26]

4. Conclusions

The semiconducting properties of the titanium oxide films formed on titanium were investigated. It has been demonstrated that the method based on electrochemical impedance spectroscopy (EIS) can yield the flat band potential and donor densities in the oxide film. The flat band potential varies with pH of the solution. As compared with our previous study [28] the flat band potential decreases as pH of the solution increases. The comparison of donor densities with the film formation potential suggests that donor density is decreasing with increasing potential. This may mean that at higher formation potentials the oxide grown on the metal surface has less defects. Since at constant potential there is virtually no change in donor densities with the variation of pH in the range from 2.9 to 8.9 [28] one can deduce that anodization potential is the convenient parameter to change donor densities. Detected n-type conductivity speaks for the presence of oxygen vacancies and Ti^{3+} ions as electron donors in TiO_2 thin films. Since the redox reactions that may occur on the oxide surface are related to the electrical properties of the film, it may help to understand its stability during contact with different environment.

Acknowledgements

The authors are grateful to Prof. Joop Schoonman from Delft University of Science and Technology in whose laboratory impedance measurements were carried out. This work was supported by the Polish Ministry of Science and Higher Education under grant No. N507 190 32/2954.

REFERENCES

- [1] J. A. Helsen, H. J. Breme, *Metals as Biomaterials*, John Wiley & Sons, England, 1998.
- [2] J. Grauman, T. Say, *Advanced Materials and Processes* **3**, 25 (2000).
- [3] K. Azumi, M. Seo, *Corros. Sci.* **45**, 413 (2003).
- [4] T. Ohtsuka, N. Nomura, *Corros. Sci.* **39**, 1253 (1997).
- [5] Z. Tun, J. J. Noel, D. Shoosmith, *J. Electrochem. Soc.* **146**, 988 (1999).
- [6] M. Harranen, J. O. Carlsson, *Corros. Sci.* **43**, 365 (2001).
- [7] H. C. Cheng, S. Y. Lee, C. C. Chen, Y. C. Shyng, K. L. Ou, *J. Electrochem. Soc.* **154**, E13 (2007).
- [8] J. W. Schultze, M. M. Lohrengel, *Electrochim. Acta* **45**, 2499 (2000).
- [9] M. Saitou, *J. Phys. Chem. B* **108**, 12170 (2004).
- [10] P. R. F. Barnes, L. K. Randeniya, P. F. Vohralik, I. C. Plumb, *J. Electrochem. Soc.* **154**, H249 (2007).
- [11] K. Azumi, M. Seo, *Corros. Sci.* **3**, 533 (2001).
- [12] V. Zwilling, E. Darque-Ceretti, A. Boutry-Forveille, D. David, M. Y. Perrin, M. Aucouturier, *Surf. Interface Anal.* **27**, 629 (1999).
- [13] A. G. Munoz, *Electrochim. Acta* **52**, 4167 (2007).
- [14] B. O'Regan, M. Gratzel, *Nature* **353**, 737 (1991).
- [15] A. Fujishima, K. Honda, *Nature* **238**, 37 (1972).
- [16] A. Fujishima, X. Zhang, C. R. Chimie **9**, 750 (2006).
- [17] I. U. Petersson, J. E. L. Loberg, A. S. Fredriksson, E. K. Ahlberg, *Biomaterials* (2009), doi:10.1016/j.biomaterials.2009.05.042
- [18] D. Landolt, *Corrosion and Surface Chemistry of Metals*, CRC Press, 2007.
- [19] O. Blum, U. Konig, *Appl. Surf. Sci.* **86**, 417 (1995).
- [20] M. Pourbaix, *Atlas of Electrochemical Equilibria in Aqueous Solutions*, NACE, 1974.
- [21] E. Barsoukov, J. R. Macdonald ed.: *Impedance Spectroscopy – Theory, Experiment and Applications*, Wiley-Interscience, Chichester 2005.
- [22] M. E. Orazem, B. Tribollet, *Electrochemical Impedance Spectroscopy*, John Wiley & Sons, Hoboken, New Jersey 2008.
- [23] S. V. Gnedenkov, S. L. Sinebryukhov, V. I. Sergienko, *Russ. J. Electrochem.* **42**, 197 (2006).
- [24] V. Macagno, J. W. Schultze, *J. Electroanal. Chem.* **180**, 157 (1984).
- [25] J. Pan, D. Thierry, C. Leygraf, *J. Biomed. Mat. Res.* **28**, 113 (1994).
- [26] H. O. Finklea, *Semiconductor electrodes*, Elsevier, New York, (1988).
- [27] A. Goossens, *Surf. Sci.* **365**, 662 (1996).
- [28] P. Handzlik, K. Fitzner, *Arch. Met. Mat.* **52**, 543 (2007).